arXiv:1302.4514v1 [cond-mat.mes-hall] 19 Feb 2013

Engineering three dimensional topological insulator in Rashba-type spin-orbit coupled heterostructure

Tanmoy Das[1], A. V, Balatsky[1,2,3]
[1]Theoretical Division, Los Alamos National Laboratory, Los Alamos, NM 87545, USA
[2]Center for Nanotechnology, Los Alamos National Laboratory, Los Alamos, NM 87545, USA.
[3]Nordita, Roslagstullsbacken 23 , 106 91 Stockholm Sweden.

(Dated: February 20, 2013)

Topological insulator represents a new class of quantum phase defined by invariant symmetries and spin-orbit coupling that guarantees metallic Dirac excitations at its surface. The discoveries of these states have sparked the hope of realizing nontrivial excitations and novel effects like magnetoelectric effect and topological Majorana excitations. Here we develop a theoretical formalism to show that three dimensional topological insulator can be designed artificially via staking bilayers of two-dimensional Fermi gases with opposite Rashba-type spin-orbit coupling on adjacent layers, and with inter-layer quantum tunneling. We demonstrate that in the stack of bilayers grown along (001)-direction a nontrivial topological phase transition occurs above a critical number of Rashba-bilayers. In the topological phase we find the formation of a single spin-polarized Dirac cone at the Γ-momentum point. This approach offers an accessible way to design artificial topological insulators in a set up that takes full advantage of atomic layer deposition approach. This approach also allows us to bypass limitations imposed by bulk crystal geometry and is tunable.

The unusual properties of topological insulator (TI) rely on searching suitable materials that inherit invariant symmetries and spin-orbit coupling in the bulk ground state, and that allow the formation of metallic Dirac fermions at the boundary.[1–6] From theoretical standpoint, the bulk symmetries include combination of low-lying odd parity orbitals, and time-reversal symmetry with a crystal geometry that can conspire an inverted band structure via strong spin-orbit coupling,[2, 8] or sometimes crystal mirror symmetry.[3] The main focus of the search of TIs is thus limited on synthesis of bulk materials with these inherent characteristics. Compounds of choice are the ones (Bi-based compounds[9, 10] and their potential functional variants[3, 11–13]) with large bulk spin orbit insulating gap. The efforts have then been extended to manipulating the 'non-trivial' topological phase by driving a trivial topological system through topological phase transition via chemical doping,[14, 15] or by tuning lattice constant,[13] or by introducing broken symmetry quantum phases.[16, 17] These materials offer tremendous opportunity for application as well as realization of numerous nontrivial properties such as anti-localization, unusual magneto-electric effect, fractional quantum statistics, and controlled electronic mass by applied magnetic field, or proximity to quantum orders.[1, 2, 18–21] Yet, as exciting as these possibilities are, exposing the Dirac cone to the bulk insulating gap or even sometimes obtaining true bulk insulator have remained uncharted, and thus pose an active topic of intense research.

We propose here an alternative approach to design TIs by combining a set of layers of two dimensional Fermi gases (2DFGs) with Rashba-type spin-orbit coupling. The surface spin-orbit locked metallic state, in the presence of interlayer quantum tunneling, translates into a bulk insulator with Z_2-invariant topological properties, with Dirac excitations on the surface. The idea is to grow two counter-helical Rashba-planes ('Rashba-bilayer') $-$ which hitherto imposes time-reversal invariance $-$ along the (001)-axis with an interlayer distance that enables single-electron hopping between them. With an effective Hamiltonian, we observe that above a critical number of Rashba-bilayers, about 5-6 layers for a realistic parameter choice, the non-trivial TI phase emerges. The resulting gapless single-Dirac cone has a linear slope determined by the bulk Rashba-coupling strength, and thus tunable internally and externally. With the rapid expansion of surface growth techniques like molecular beam epitaxy, one would be able to explore a large set of compounds that might not be accessible in the bulk phase, and yet possess TI behaviors. We find that this 'layer by layer' approach of Rashba-bilayers has all the same known set of properties as the bulk TI; for example we present a direct calculation of the Chern index in the bulk to support the topological nature of the resultant state. With the rapid expansion of surface growth techniques like molecular beam epitaxy, one would be able to explore a large set of compounds that might not be accessible in the bulk phase, and yet possess TI behaviors.

In what follows, we lay a general framework for generating and manipulating 'homemade' three dimensional TI. The presence of Dirac cone at the Fermi level without the intervention of bulk state will also make it a attractive candidate to realize the fractional statistics and non-Abelions.[1, 2] In principle one can envision to use the approach we propose and take it few steps further, e.g. it allows one to introduce layers of magnetic,[20, 21] superconducting[18, 19, 22] and other many body orders[23] within the topological matrix. Taken together, the search for TI materials which obey several symmetry properties and inherits spin-orbit coupling can thus be replaced with 'homemade' systems by generating spin-orbit coupling via external electron field, and imposing symmetry properties via manipulating heterostructure geometry which will be free from any particular crystal geometry.[24]

Rashba-bilayer heterostructure

We start with depicting our basic idea in Fig. 1, and constructing the low-energy effective Hamiltonian. The cornerstone of this framework relies on gluing two counter-propagating Rashba-type spin-orbit coupled 2DFGs, denoted by $\pm\alpha(\boldsymbol{k})$, close to each other such that finite quantum tunneling $[D(\mathbf{k})]$ is activated between them, as illustrated in Fig. 1a. Such Rashba-bilayer can easily be manufactured by creating potential gradient between two 2DFGs with the help of gating, or by inserting polarized medium between them, among others. As opposed to a metallic single-Rashba 2DFG, the Rashba-bilayer governs an insulating gap, determined by the value of $D(\mathbf{k})$, with a minimum gap at the Γ-momentum point. Then Rashba-bilayers can be grown along (001) direction with an inter-bilayer electron hopping, t_z, which is required to be different than $D(0)$ to eliminate the degeneracy in the band structure. Above a critical number of the Rashba-bilayers in such heterostructure setup, a bulk topological phase transition commences, which turns the quantum well band curvature into an inverted band dispersion or 'dent' structure in the valence Fermi sea, as illustrated in Fig. 1d. Such inverted band dispersion is also observed in first-principles band structure calculations,[25] and angle-resolved photoemission spectroscopy (ARPES) measurements[14] in 3D bulk materials. Both analytically and numerically, we investigate below a widespread realistic parameter space in which a non-trivial topological phase transition is governed with single Dirac cone, carrying all salient topological properties that are derived and realized earlier in bulk three-dimensional systems.[1, 2] A detailed progression of the resulting band structure is given in the supplementary information (SI).

Effective model of Rashba-bilayer heterostructure

Based on the above-proposed setup, we now derive an effective low-energy theory for the origin of TI. For each 2DFG planes, an electron with momentum $\boldsymbol{k}$ experiences an effective 'anisotropic' magnetic field, induced by an electric field $\boldsymbol{E}_z$, which couples to its spin $\boldsymbol{\sigma}$ to give rise to Rashba-type spin-splitting electronic bands $h_R^{\pm} = k^2/2m^* \pm \alpha_R(\boldsymbol{k}\times\boldsymbol{\sigma})$, where α_R is Rashba-coupling strength, controlled by external or internal electric field, and m^* is the effective mass of electrons. $\boldsymbol{k}$ is defined in the 2D plane, and correspondingly $\boldsymbol{\sigma}$ stands for Pauli matrices in the spin-subspace. We take two such counter-propagating helical 2DFGs, h_R^+ and h_R^-, close to each other, either on the same plane or out of plane, such that finite quantum tunneling $D(\boldsymbol{k})$ between them becomes active. Then this setup is grown along $z-$axis with a non-spin-flip electron hopping between them, t_z. Therefore, the general form of the effective Hamiltonian for N number of semi-infinite layers within open-boundary condition can be expressed as

$$H = \begin{pmatrix} h_R^+ & D & \mathbf{0} & \mathbf{0} & \ldots \\ D & h_R^- & T & \mathbf{0} & \ldots \\ \mathbf{0} & T & h_R^+ & h_{12} & \ldots \\ \mathbf{0} & \mathbf{0} & h_{12} & h_R^- & \ldots \\ \vdots & \vdots & \vdots & \vdots & \ddots \end{pmatrix} \tag{1}$$

Each term in the above Hamiltonian is a 2×2 matrix. To keep the formalism general and readily tunable, we take 'anisotropic' hoppings between h_R^+ and h_R^- as $D(\boldsymbol{k}) = (D_0 + Mk^2)\mathrm{I}_{2\times2}$, which can also be thought of as Dirac mass and Newtonian mass, respectively, due to their fundamental impacts on the obtained band structure. The tunneling between two adjacent bilayers is $T = t_z\mathrm{I}_{2\times2}$. $\mathbf{0}$ is a 2×2 component zero vector and $\mathrm{I}_{2\times2}$ is the identity matrix. Time-reversal invariance of the above Hamiltonian consequently emerges due to the fact that $h_R^{-\dagger}(-\boldsymbol{k}) = h_R^+(\boldsymbol{k})$, which is an essential criterion for the formation of helical edge state, endowing the system to Z_2 classification.[2, 4–6, 8, 26]

The values of parameters m^* and α_R depend on the type of Rashba-setup under consideration, whereas those for the expansion parameters D, M and t_z are controllable mainly by the details of the heterostructure. An elaborated band structure progression as a function of these parameters is given in *SI*. Here we discuss the emergence of topological bulk insulator with helical surface state for a representative value of $m^* = 0.1$ eV^{-1}Å^{-2}, and $\alpha_R = 1.5$ eVÅ. Such value and even higher value of Rashba parameter is readily achievable in Bi-based surface and quantum-well states, as well as in BiTeI bulk systems.[3] The Dirac mass has the same meaning as used for 2D quantum spin Hall (QSH) insulator,[28] and 3D TIs,[8] in that it is responsible for opening a band gap between the two adjacent time-reversal terms h_R^+ and h_R^- at the Γ-point inside the bulk setup. When several slabs of two 2DFGs are glued together with t_z, the insulating gap persists in every layers except on the boundary. Two helical edge states develop at each boundary which meet at a gapless Dirac cone above a critical value of the number of layers, N_c.

The value of N_c depends only on the Dirac mass term D_0 and on interlayer tunneling t_z, but not on other terms, and thus controllable solely by the 'layer-by-layer' deposition procedure. We illustrate this case for a representative value of $D_0 = -25$ meV, $t_z = -0.2$ eV in Fig. 2. Above three or more layers of Rashba-bilayers, we observe, both numerically and analytically (see SI), that an inverted bulk insulating gap develops in the interior Rashba-bilayers, which reflects in the transformation of the quantum-well-like states of the inherent slabs into inverted dispersions resembling a 'dent' shape in the filled Fermi sea. We recall that this 'dent'-like inverted valance band is a critical signature of non-trivial topological phase, and has been consistently evaluated via first-principles calculations,[25] and also been observed in 3D TI materials.[14]

To further quantify the 'strong' topological phase transition as a function of number of layers, we also compute the topological invariants ν (or equivalently an axion angle parameter θ) of the Hamiltonian in Eq. (1). Since the Hamiltonian is invariant under inversion symmetry, we can derive the essential parity operator for each pair of Kramers degenerate valence bands from the constraint $PH(k)P^{-1} = H(-k)$, with $P = \sigma_z \otimes I_{2\times 2}$, for each Rashba-bilayers. Thus we evaluate the topological quantum index as[29]

$$(-1)^{\nu} = \prod_{i} \prod_{l=1}^{N} \langle \phi_l | P | \phi_l \rangle, \tag{2}$$

where i stands for the the time-reversal high-symmetry points on the Brillouin zone, and ϕ_l is the eigenvector for each layer l. For the parameter set, we indeed find that a parity inversion occurs at N_c, which, according to Z_2 topological criterion,[2, 4, 8, 26] marks the emergence of topological insulating phase at this critical value of N. Above this critical thickness, the parity value stabilies to the non-trivial TI.[30]

A consequence of the Z_2 TI is the presence of spin-polarized Dirac cone at the surface. Despite the emergence of 'non-trivial' topological phase above three bi-layers, a surface gap persists due to finite quantum tunneling between the two edges, and the massless Dirac point disappears above five layers for this parameter choice. Such formation of massive Dirac quasiparticles below a critical value of quintuple layers is observed in Bi_2Se_3 thin films,[22] and also in doped bulk $TlBi(S_{1-x}Se_x)_2$[14, 15].

We tabulate the values of bulk and surface gaps as a function of various tuning parameters in Fig. 3. As expected the electron's mass m^* and Rashba-coupling α_R do not have significant effect on the gap values, and thus gives us an alternative approach for generating bulk TI beyond atomistic spin-orbit coupling and heavy electron mass. The Dirac mass D and interlayer tunneling provide the backbone for engineering the surface and bulk gaps, which are readily tunable via heterostructure details. In *SI*, we show the corresponding energy dispersions.

Surface Dirac cone properties

We can formulate the Hamiltonian for the the edge state by using the theory of invariants. The time-reversal symmetry imposes that a spin-up state at momentum $\boldsymbol{k}$ must be entangled to a state with spin-down at $-\boldsymbol{k}$ via spin-orbit coupling. As a consequence of this, according to Fermion doubling theorem, gapless Dirac point is guaranteed at Γ-point. In what follows, two counter-propagating surface states form with one spin state from the upper Rashba-term (h_R^+), and an opposite spin state from the lower Rashba term (h_R^-), which are related by time-reversal operation. By projecting the full Hamiltonian in Eq. 1 onto a single slab, we can write down the surface Hamiltonian in this basis to the leading order in k as

$$H_{surf} = \alpha_R(\sigma^x k_y - \sigma^y k_x). \tag{3}$$

Note that the similar surface dispersion is also obtained on 3D TI in Refs. [2, 8], except that here its slope is solely determined by the Rashba-coupling strength. Therefore, the velocity of the Dirac fermions turns out to be $v = \alpha_R/\hbar$, and thus externally tunable. For the value of Rashba-coupling constant as large as 3.8 eV$\mathring{A}$ achieved to date in bulk BiTeI,[3] we get $v \simeq 5.8 \times 10^5$ m/s, which is even larger than the value achieved to date in a 3D

TIs.[9, 31] The deviation from the linear slope of the surface state within the bulk insulating gap depends on the value of mass term $D(0)$. For the parameter set used above, we obtain linear dispersion expanding about 0.3 eV on both sides of the Dirac point, which is also tunable (see *SI*).

The spin-polarized surface states can be imaged directly by ARPES and tunneling spectroscopies, as well as via transport measurements. An interesting transport parameter of Dirac fermions is the quantum Hall effect which can be achieved by inserting a magnetic layer in the heterostructure next to the boundary, so that it breaks time-reversal symmetry on the surface via proximity effect, but not in the bulk.[2, 20] We can express the surface and magnetic layer Hamiltonian in a combined 'd'-vector form as $\boldsymbol{d}\cdot\boldsymbol{\sigma}$, where the time-reversal invariant components are $d_x = -\alpha_R k_x$ and $d_y = \alpha_R k_y$, and time-reversal breaking d_z gives the Zeeman energy splitting due to induced magnetization. Without the presence of a d_z term, the winding number of the upper and lower chiral states, defined as $C = \frac{1}{4\pi^2}\int dk_x \int dk_y \hat{d}\cdot(\partial_x\hat{d}\times\partial_y\hat{d})$ (the notation 'hat' represents corresponding unit vector) where the integration is performed in closed loop around the Dirac cone, cancel each others. However, when a broken time-reversal symmetry is imposed, C becomes equal to $\pm\sigma_z$, where σ_z is the component of the spin along the magnetic field orientation. In this case, QSH conductance becomes fractional in units of e^2/h as $\sigma_H = \mp(|\sigma_z|/2)(e^2/h)$. For fully polarized spin-configuration along the magnetic field, the above equation generates half-integer anomalous quantum-Hall effect (QHE). The fractional or half-integer QHE is a trademark feature of Dirac systems,[1, 2, 31, 32] and can be used as a test of our proposal from transport perspective. An interesting consequence of the half-integer landau level is that as TR breaking mass term, d_z, approaches zero, the counter-propagating Landau levels move to zero energy, and the system can act as protected quantum Hall 'insulator' despite the presence of energy states at the Fermi energy[33]. This unique scenario has been discussed theoretically for TIs, but never been realized experimentally due to the absence of isolated Dirac point at E_F,[31] however, it can be realized in the present heterostructure setup.

Outlook

Our proposal clearly overcomes the limitation of searching suitable combinations of crystal geometry, and inherent wave function symmetries within a bulk system for the material realization and device implementation of the topological properties. The present formalism is free from any particular crystal geometry, and thus provides a widespread playground for engineering 'homemade' TI and surface state properties. Another advantage of the present case is that here the edge state is exposed to the bulk insulating gap, instead of being buried inside the bulk Fermi sea, which has greatly limited the usage of existing 3D TIs. The heterostructure, with depositing capability of one atomic layer at a time, can also accommodate magnetic and superconducting layers, beyond the conventional doping or proximity effects, and thus will promote a unambiguous detection of non-Abelian particles such as 'axions', Majorana fermions[18, 20, 21] without the distraction of vortex, impurity, or dopant states. Given that electron interaction is stronger in 2DFG,[23] novel broken symmetry phases are easy to yield inherently in its heterostructure than in a weakly correlated 3D TI.

We are indebted to S. Basak and A. M. Black-Schaffer for numerous discussions. This work was supported, in part, by UCOP and by Los Alamos National Laboratory, of the US Department of Energy under Contract DE-AC52-06NA25396, VR and ERC, and benefited from the allocation of supercomputer time at NERSC.

---

[1] Hasan, M. Z. & Kane, C. L. Colloquium: TIs. *Rev. Mod. Phys.* **82**, 3045-3067 (2010).

[2] Qi, X-L. & Zhang, S-C. TIs and superconductors. *Rev. Mod. Phys.* **83**, 1057-1110 (2011).

[3] Fu, L. Topological crystalline insulators. *Phys. Rev. Lett.* **106**, 106802 (2011).

[4] Roy, R. Z_2 classification of quantum spin Hall systems: An approach using time-reversal invariance. *Phys. Rev. B* **79**, 195321 (2009).

[5] Schnyder, A. P., Ryu, S., Furusaki, A. & Ludwig, A. W. W. Classification of TIs in three spatial dimensions. *Phys. Rev. B* **78**, 195125 (2008).

[6] Slager, R.-J., Mesaros, A., Juricic A., & Zaanen J. The space group classification of topological band insulators. *Preprint available at http://arxiv.org/abs/1209.2610.* Accepted in Nat. Phy. (2012).

[7] Fu, L., Kane, C. L., & Mele, E. J. TIs in three dimensions. *Phys. Rev. Lett.* **98**, 106803 (2007).

[8] Zhang, H. *et al.* TIs in Bi_2Se_3, Bi_2Te_3 and Sb_2Te_3 with a single Dirac cone on the surface. *Nat. Phys.* **5**, 398 (2009).

[9] Xia, Y. *et al.* Observation of a large-gap topological-insulator class with a single Dirac cone on

the surface . *Nat. Phys.* **5**, 398-402 (2009).

[10] Chen, Y. L. *et al.* Experimental realization of a three-dimensional TI Bi_2Te_3. *Science* **10**, 325 (2009).

[11] Lin, H. *et al.* Half-Heusler ternary compounds as new multifunctional experimental platforms for topological quantum phenomena. *Nat. Mat.* **9**, 546-549 (2010).

[12] Chadov, S. *et al.* Tunable multifunctional TIs in ternary Heusler compounds. *Nat. Mat.* **9**, 541-545 (2010).

[13] Lin, H. *et al.* Single-Dirac-cone Z_2 TI phases in distorted Li_2AgSb-class and related quantum critical Li-based spin-orbit compounds. *Preprint available at http://arxiv.org/abs/1004.0999.*

[14] Xu, S.-Y. *et al.* Topological phase transition and texture inversion in a tunable TI *Science* **332**, 560 (2011).

[15] Sato T. *et al.*, Unexpected mass acquisition of Dirac fermions at the quantum phase transition of a TI. *Nat. Phys.* **7**, 840 (2012).

[16] Raghu, S. *et al.* Topological mott insulators. *Phys Rev Lett.* **100**, 156401 (2008).

[17] Mong, R. S. K., Essin, A. M., & Moore J. A. Antiferromagnetic TIs Phys. Rev.B **81**, 245209 (2010).

[18] Fu, L. & Kane, C. L. Probing neutral Majorana fermion edge modes with charge transport. *Phys. Rev. Lett.* **102**, 216403 (2009).

[19] Linder, J. *et al.* Unconventional superconductivity on a TI. *Phys. Rev. Lett.* **104**, 067001 (2010).

[20] Qi, X-L., Li, R., Zang, J., & Zhang, S.-C. Inducing a magnetic monopole with topological surface states. *Science* **323**, 1184-1187 (2009).

[21] Essin, A., Moore, J. E. & Vanderbilt, D. Magnetoelectric polarizability and axion electrodynamics in crystalline insulators. *Phys. Rev. Lett.* **102**, 146805 (2009).

[22] Wang M.-X. *et al.* The coexistence of superconductivity and topological order in the Bi_2Se_3 thin films, *Science* **336**, 52 (2012).

[23] Das, T. Interaction induced staggered spin-orbit order in two-dimensional electron gas. *Phys. Rev. Lett.* **109**, 246406 (2012).

[24] Qiao, Z., Tse, W.-K., Jiang, H., Yao, Y. & Niu, Q. Two-dimensional topological insulator state and topological phase transition in bilayer graphene. *Phys. Rev. Lett.* **107**, 256801 (2011).

[25] Klintenberg, M. The search for strong TIs. *Preprint available at*

http://arxiv.org/abs/1007.4838.

[26] Moore, J. E. & Balents, L. Topological invariants of time-reversal-invariant band structures. *Phys. Rev. B* **75**, 121306 (2007).

[27] Ishizaka K. *et al.*, Giant Rashba-type spin splitting in bulk BiTeI. *Nat. Mat.* **10**, 521 (2011).

[28] Bernevig, B. A., Hughes, T. L., & Zhang, S. C., Quantum spin Hall effect and topological phase transition in HgTe quantum wells. *Science* **314**, 1757 (2006).

[29] Ebihara, K., Yada, K., Yamakage, Ai, & Tanaka, Y. Finite size effects of the surface states in a lattice model of TI. *Preprint available at http://arxiv.org/abs/1111.3528.*

[30] Liu, C.-X. *et al.* Oscillatory crossover from two-dimensional to three-dimensional topological insulators. *Phys. Rev. B* **81**, 041307(R) (2010).

[31] Qu, D.-X. *et al.*, Quantum oscillations and Hall anomaly of surface state in the TI Bi_2Te_3. *Science* **329**, 821 (2010).

[32] Castro Neto, A. H. *et al.* The electronic properties of graphene. *Rev. Mod. Phys.* **81**, 109 (2009).

[33] Jackiw, R. Fractional charge and zero modes for planar systems in a magnetic field. *Phys. Rev. D* **29**, 2375 (1984).

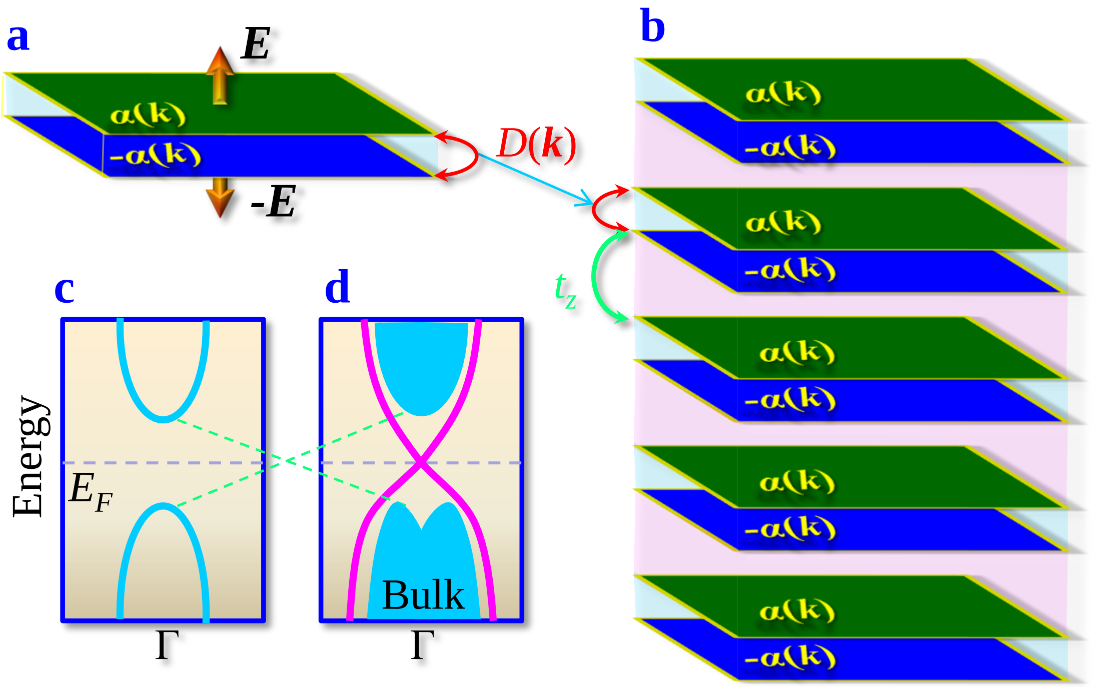

FIG. 1. **Rashba-bilayer of 2DFGs and its heterostructure setup.** **a**, A bilayer combination of opposite Rashba-type spin-orbit coupling 2DFGs, denoted by $\alpha(\boldsymbol{k})$, $-\alpha(\boldsymbol{k})$, representing h_R^+ and h_R^-, respectively in the Hamiltonian in Eq. 1. $D(\mathbf{k})$ gives the interlayer electron tunneling between them. **b**, As grown Rashba-bilayers with finite interlayer coupling, t_z. **c**, **d**, Illustration of band dispersions for a bilayer 2DFG, and its heterostructure version, respectively. The emergence of inverted band curvature in the valence bulk band marks the topological phase transition (see text).

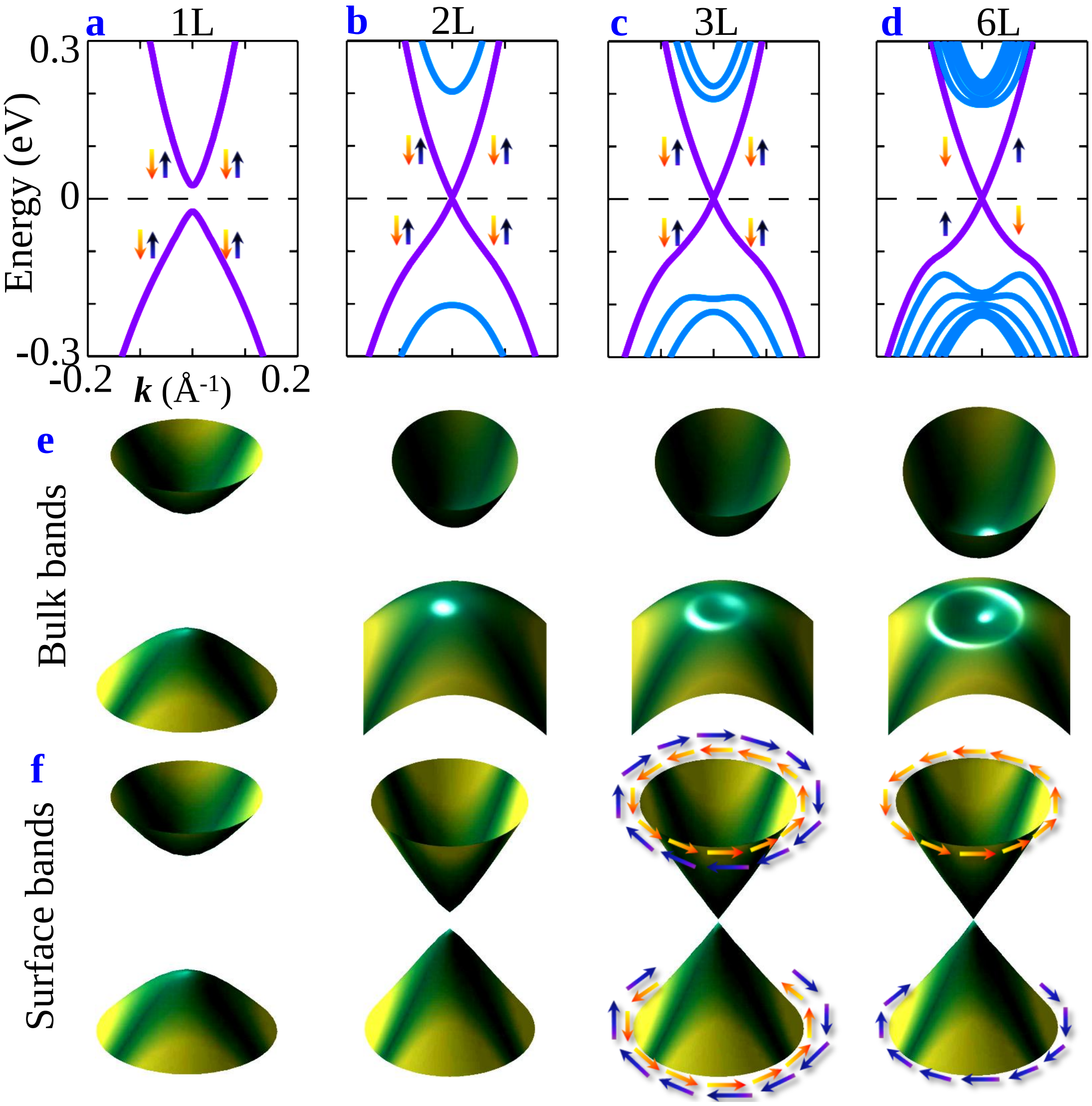

FIG. 2. **Band progression and formation of gapless surface state. a-d**, Evolution of band dispersion for single layer (1L) to six layers (6L) of Rashba-bilayer setup. **e-f**, Corresponding 3D view of the band dispersions in the k_x, k_y-plane for the bulk (top panel) and surface (bottom panel) bands, respectively. The parameter set for this calculation is given in text. In going from two to three bilayers, the bulk valence band topology reveals the emergence of an inverted shape [see also **c** and corresponding **f**], which indicates the topological phase transition from trivial to non-trivial phase. However, it takes about six bilayers to turn off the inter-edge tunneling to commence gapless Dirac cone at the surface. Arrow dictate the spin orientation. The definite spin-chirality for the gapless Dirac cone is illustrated by counter-rotating arrows in **f**.

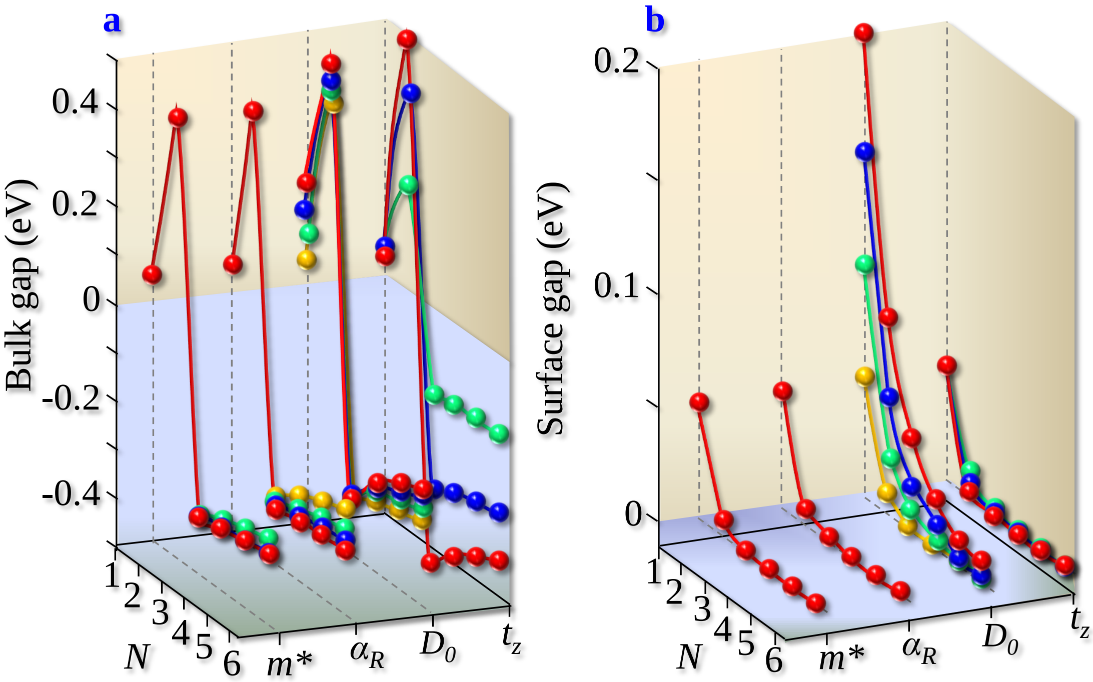

FIG. 3. **Bulk and surface gaps in a realistic parameter space.** **a**, The critical number of layers, N_c, at which an inverted bulk gap opens. The bulk band gap jumps from $D(0)$ at N=1 (equivalent to t_z=0) to a large positive value, and then consistently becomes negative for $N \geq 3$, constrained by the Hamiltonian (see *SI*). For each parameter set, the corresponding other parameters are set to be constants to the values mentioned in the main text. The varying parameters are: m^*=1 (green), 2.5 (blue), 5 (red) in eV^{-1}Å^{-2}. α_R=1 (orange), 1.5 (green), 2 (blue), and 3 (red) in eVÅwhich are attainable in existing system.[3] D_0=-25 (orange), -50 (green), -75 (blue), and -100 (red) in meV, and t_z=-10 (green), -20 (blue) and -50 (red) meV. Since $Mk^2 = 0$ at the Γ-point, the parameter M does not have any effect on the direct gap structure. **b**, Corresponding surface gaps at the Γ-point. Clearly, the gapless surface Dirac cone formation depends on two parameters, the interlayer hybridization t_z, and strongly on the Dirac mass D. The parameter values here are same as in **a**.

Supplementary Information for "Engineering three dimensional topological insulator in Rashba-type spin-orbit coupled heterostructure"

Tanmoy Das[1], A. V, Balatsky[1,2,3]
[1]Theoretical Division, Los Alamos National Laboratory, Los Alamos, NM 87545, USA.
[2]Center for Nanotechnology, Los Alamos National Laboratory, Los Alamos, NM 87545, USA.
[3]Nordita, Roslagstullsbacken 23 , 106 91 Stockholm Sweden.

BAND DISPERSIONS FOR A RASHBA-BILAYERS

In this supplementary information, we provide further insights into the emergence of TI from analytical description. The Rashba-type spin-orbit coupling splits a non-interacting band into two in-plane spin-polarized bands. To keep the formalism general, we take a two-dimension Fermi gas (2DFG), with quadratic band, $k^2/2m^*$, where m^* is the effective mass of electrons. Under Rashba-coupling,[1] the split bands are obtained by solving $h_R^{\pm} = k^2/2m^* I_{2\times 2} \pm \alpha_R(k_y\sigma_x + k_x\sigma_y)$, where α_R is Rashba-coupling. For simplicity, we define the second term as $\alpha(\boldsymbol{k})$. Next we create a bi-layer 2DFG with two counter-propagating helical 2DEGs, h_R^{+} and h_R^{-} in which finite quantum tunneling is turned on, as denoted by $D(\boldsymbol{k})$. The Hamiltonian for bi-layer 2DFG can be written explicitly as

$$H = \begin{pmatrix} k^2/m^* & \alpha(\boldsymbol{k}) & D(\boldsymbol{k}) & 0 \\ \alpha^{\dagger}(\boldsymbol{k}) & k^2/m^* & 0 & D(\boldsymbol{k}) \\ D(\boldsymbol{k}) & 0 & k^2/m^* & -\alpha(\boldsymbol{k}) \\ 0 & D(\boldsymbol{k}) & -\alpha^{\dagger}(\boldsymbol{k}) & k^2/m^* \end{pmatrix}. \tag{4}$$

The resulting eigenvalues are two-fold degenerate: $E^{\pm}(\boldsymbol{k}) = k^2/m^* \pm \sqrt{\alpha^2(\boldsymbol{k}) + D^2(\boldsymbol{k})}$. This specific bi-layer setup helps generating two upward and downward dispersing bands, with a direct gap between them defined by $D(\boldsymbol{k})$ at Γ-point (since $\alpha(0) = 0$), see Fig. S1b. $D(\mathbf{k})$ shall be even under inversion, e.g. $D(\boldsymbol{k}) = D_0 + Mk^2$, which destroys the spin-polarization, implying that the gap between the band bands is charge insulating.

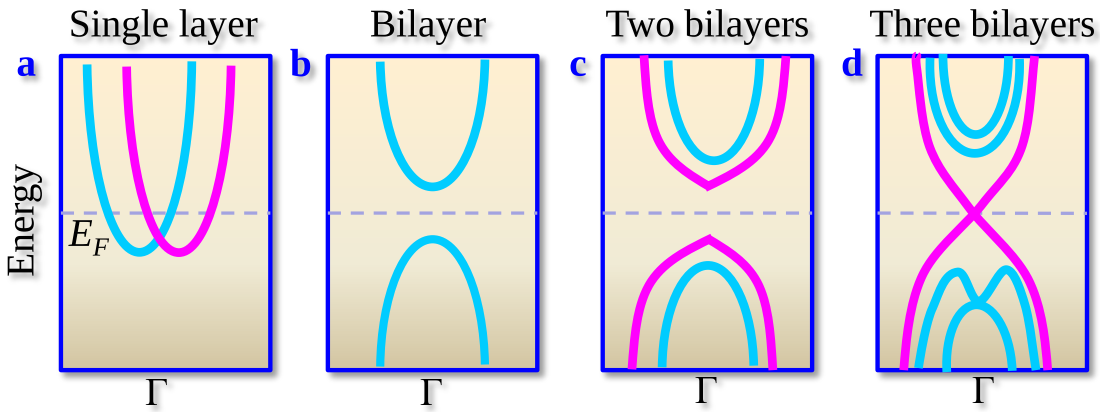

Fig. S1. Band progression from single to bilayer to heterostructure of Rashba-type spin-orbit coupling 2DFGs.

BAND DISPERSIONS FOR TWO RASHBA-BILAYERS

As depicted in Fig. 1 of the main text, we now take two bilayer 2DEG, grown along (001) direction such that quantum tunneling, say t_z, between the adjacent layers becomes active. The explicit form of the Hamiltonian for this case is

$$H = \begin{pmatrix} k^2/m^* & \alpha(\boldsymbol{k}) & D(\boldsymbol{k}) & 0 & 0 & 0 & 0 & 0 \\ \alpha^\dagger(\boldsymbol{k}) & k^2/m^* & 0 & D(\boldsymbol{k}) & 0 & 0 & 0 & 0 \\ D(\boldsymbol{k}) & 0 & k^2/m^* & -\alpha(\boldsymbol{k}) & t_z & 0 & 0 & 0 \\ 0 & D(\boldsymbol{k}) & -\alpha^\dagger(\boldsymbol{k}) & k^2/m^* & 0 & t_z & 0 & 0 \\ 0 & 0 & t_z & 0 & k^2/m^* & \alpha(\boldsymbol{k}) & D(\boldsymbol{k}) & 0 \\ 0 & 0 & 0 & t_z & \alpha^\dagger(\boldsymbol{k}) & k^2/m^* & 0 & D(\boldsymbol{k}) \\ 0 & 0 & 0 & 0 & D(\boldsymbol{k}) & 0 & k^2/m^* & -\alpha(\boldsymbol{k}) \\ 0 & 0 & 0 & 0 & 0 & D(\boldsymbol{k}) & -\alpha^\dagger(\boldsymbol{k}) & k^2/m^* \end{pmatrix}. \tag{5}$$

The eigenvalues of Eq. 5 is given by

$$E^{\pm}_{\pm}(\boldsymbol{k}) = \frac{k^2}{m^*} \pm \frac{1}{2}\left[2t_z^2 + 4\left(\alpha^2(\boldsymbol{k}) + D^2(\boldsymbol{k})\right) \pm 2t_z\sqrt{t_z^2 + 4D^2(\boldsymbol{k})}\right]^{1/2}. \tag{6}$$

The energy dispersions imply that whereas a large bulk gap opens between E^+_+ and E^-_-, the gap between the lowest energy states E^+_- and E^-_+ decreases from their single bilayer value of D_0. Although, mathematically, there exists a solution for the values of D_0 and t_z at which surface gap can be closed, but there is no clear evidence of the bulk band party inversion for this Hamiltonian, and thus the resulting solution remains trivial topological phase. The absence of band inversion is also evident in the parity calculation and the parabolic shape of band dispersion as presented in the main text.

BAND DISPERSIONS FOR THREE RASHBA-BILAYERS

With three or more bilayers, coupled by finite quantum tunneling, the bulk systems begin to form in which the interior bilayer(s) acts as bulk where the edge layers give rise to surface states. We show here for three bilayers, a bulk band inversion occurs and thus promotes non-trivial topological insulating phase. However, to get rid of the electron hopping from the two edges, or in other words, to close the surface gap, one requires a higher number of bilayers.

The analytical solution gradually becomes complicated and long with further increase of bilayers. However we can gain some insights into how an inversion occurs in three bilayers of 2DFGs by the symmetry of the Hamiltonian, irrespective of parameter choices. The Hamiltonian can be easily generalized from Eq. 5, and we present the eigenvalue for some of the relevant bulk bands as,

$$E^{\pm}(\boldsymbol{k}) = \frac{k^2}{m^*} \pm \frac{1}{3X(\boldsymbol{k})}\Big[3\left(3\alpha^2(\boldsymbol{k}) + 2t_z^2 + 3D(\boldsymbol{k})\right)X^2(\boldsymbol{k}) + 6t_z^2\left(t_z^2 + 6D(\boldsymbol{k})\right)X(\boldsymbol{k}) \\ +6\left(3Y(\boldsymbol{k}) - 2\right)t_z^6 + 54t_z^4D^2(\boldsymbol{k})\Big]^{1/2}, \tag{7}$$

where

$$X(\boldsymbol{k}) = t_z\left[-8t_z^2 + 36t_zD(\boldsymbol{k}) + 12Y(\boldsymbol{k})\right]^{1/3},$$

and

$$Y(\boldsymbol{k}) = D(\boldsymbol{k})\left[-96D^4(\boldsymbol{k}) - 39t_z^2D^2(\boldsymbol{k}) - 12t_z^4\right]. \tag{8}$$

The important message of Eq. 7 is that there is a prefactor $1/X \sim 1/t_z(...)$ which enables an inverted band gap opening for a negative value of t_z. The resulting parity inversion in the valence band endows a non-trivial topological phase transition at a large parameter space (see Fig. 3 of main text). A visual proof of the inverted band gap can be obtained from the associated inverted band curvature of 'dent' shape in the valence bulk band, as illustrated in Fig. S1c. According to Fu-Kane criterion,[2] for such case gapless Dirac states appear at the surface. However, for most values of the parameters shown in supplementary Fig. S2, finite gap at the surface still persists due to finite size-effect, and the surface gap closing requires characteristic number of layers of Rashba-bilayers.

DEPENDENCE OF BULK AND SURFACE BAND STRUCTURE ON VARIOUS PARAMETERS

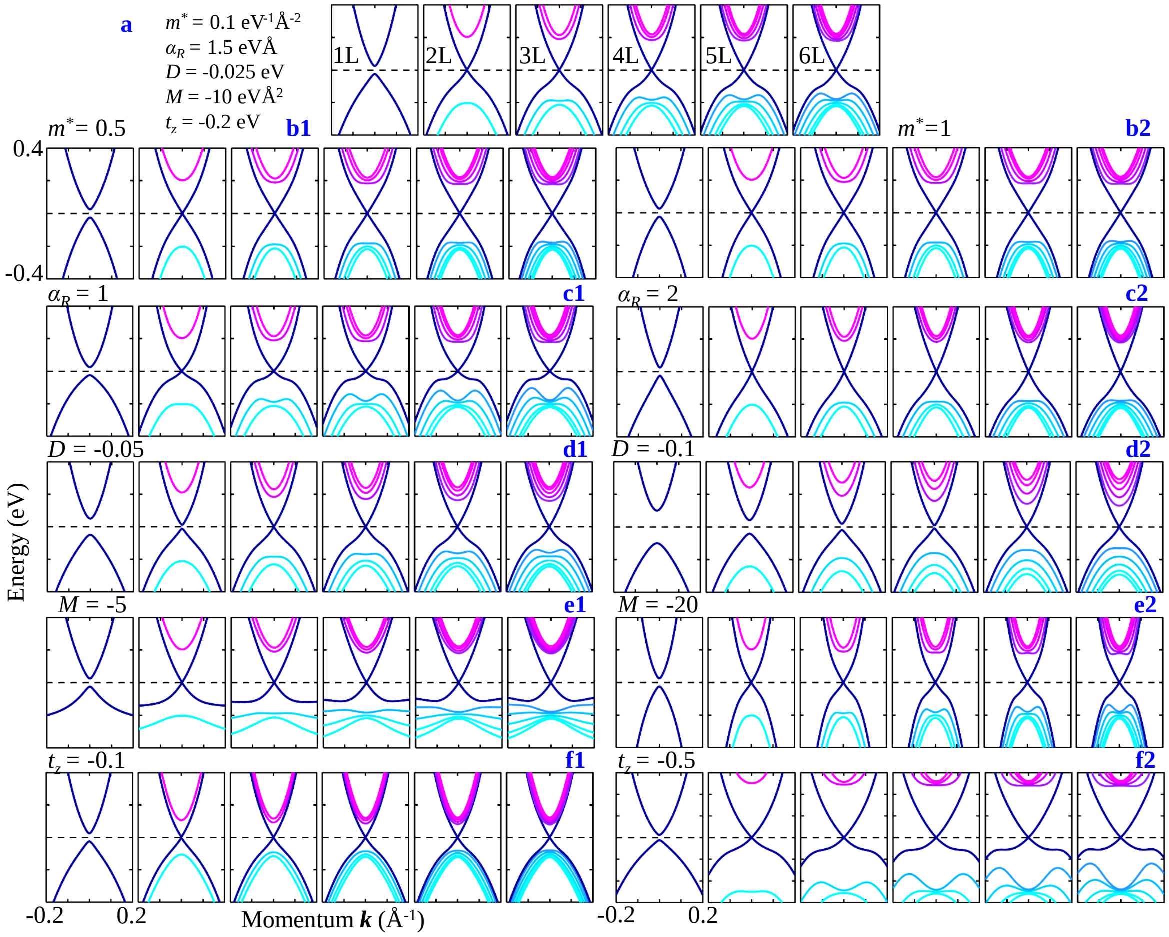

Fig. S1. Variations of dispersion relation for a wide range of parameter space. a, The band dispersion for a bilayer 2DFG to six layers setup as shown in Fig. S1 of the main text. In the rest of the figures, only a single parameter is tuned (in each row), while keeping others parameters same to that in **a**. In each figures, the horizontal axis spans within k_x = -0.2 to 0.2 Å^{-1} with $k_y = 0$ and the vertical axis runs from E =-0.4 to 0.4 eV with Fermi level (E_F) lying at the center (black dashed line), except in **f2**, where the energy scale runs from -0.6 to 0.6 eV. The value of N_c for the formation of gapless surface state depends only on t_z and D_0, whereas the slope of the surface state is controlled by the Rashba-coupling α_R (compare **b**, **c1**, and **c2**), and the span of the linearly dispersing surface state depends on the bulk insulating gap, as well as on the Newtonian mass M, as expected form Eq. 2 of the surface Hamiltonian.

For the benefit of understanding the role of each parameter on the bulk and surface band structures, and also for the purpose of material growth, we present results for systematic tuning of various parameters as a function of number of layers in Fig. S2. The same results present in Fig. 2 of the main text is reproduced here in Fig. S2a and the parameters are listed in the left side of this panel. For each row in the figures below, a single parameter is tuned while the others are kept to the value listed in Fig. S2a. The effective mass, m^* of the electrons does have any significant effect neither on the bulk and surface band-structure, nor on the slope of the emergent surface state. Since this quadratic term goes to zero at the Γ-term, it begins to play a role at higher-energy, and with increasing m^*, it only slightly reduces the indirect bulk gap. The Rashba-coupling strength α_R, as for m^*, has no role to the surface and bulk gaps (very minor contribution to the indirect bulk gap). However, as deduced in the main text in Eq. 3, α_R determines the velocity of the Dirac fermions on the surface. Since α_R is easily tunable both externally and internally, as well as, a large value of it can nowadays be achieved in available materials,[3] obtaining spin-polarized Dirac excitations with larger velocity than the presently known bulk 3D TI is possible.

The Dirac mass D_0 modifies the band gap as its definition implies, in that it controls the surface gap, however, it does not have significant effect on the bulk gap. The band curvature of the surface state also remains very much unaltered. The Newton mass M is associated with a quadratic momentum dependence, and thus does not participate in the gap, and it contributes at high-energy. Higher the value of M, better the band topology. The inter-bilayer tunneling t_z contributes almost oppositely to that of Dirac mass D_0, in that it modulates the bulk gap, however, it does not any prominent effect on the surface gap.

[1] Bychkov, Y. A. & Rashba, E. I. Properties of a 2D electron gas with lifted spectral degeneracy. *JETP Lett. 39*, 78-81 (1984).

[2] Fu, L., Kane, C. L., & Mele, E. J. TIs in three dimensions. *Phys. Rev. Lett.* **98**, 106803 (2007).

[3] Ishizaka K. *et al.*, Giant Rashba-type spin splitting in bulk BiTeI. *Nat. Mat.* **10**, 521 (2011).